iJRASET
International Journal For Research in Applied Science and Engineering Technology

INTERNATIONAL JOURNAL FOR RESEARCH

IN APPLIED SCIENCE & ENGINEERING TECHNOLOGY

Volume: 11 **Issue:** V **Month of publication:** May 2023

DOI: https://doi.org/10.22214/ijraset.2023.51080

www.ijraset.com

Call: 08813907089 | E-mail ID: ijraset@gmail.com

International Journal for Research in Applied Science & Engineering Technology (IJRASET)
ISSN: 2321-9653; IC Value: 45.98; SJ Impact Factor: 7.538
Volume 11 Issue V May 2023- Available at www.ijraset.com

Application of Aeromagnetic Data Analysis and Interpretations to Investigate Solid Mineral Potential in Part of Bauchi, Northeast Nigeria

Mustapha Babagana[1], Fatima M. Shehu[2], El-Yakub A. Idris[3], Ibrahim M.Muhammad[4], Shehu Suraju[5], Abubakar Nuhu[6], Abdullah Habib[7], Fatima Tahir Hamza[8]
[1, 2, 4, 5, 6, 7, 8]*Advanced Space Technology Application laboratory, (ASTAL), BUK, Kano*
[3]*National Metallurgical Development Center, (Jos, Nigeria)*

Abstract: ***The distribution of surface and subsurface magnetic materials within the study area, the delineation of geologic lineaments, and an estimate of the depth to magnetic sources were all determined by interpreting high resolution aeromagnetic data that covered a portion of Bauchi, northeastern Nigeria, lying between Latitudes 9040'00"N to 10010'0"N and Longitudes 900'0"E to 9040'0'E. The Aeromagnetic map, analytical signal, and horizontal derivative filters used on total magnetic intensity data after reduction to the magnetic equator (RTE) show that the Toro and its environs contain highly magnetic minerals thought to be potential deposits of iron ore. The lithological map and the lineament maps have a good connection. Further examination of the findings reveals that the research area has varying degrees of Ferro-, para-, and diamagnetic mineralization (of the iron and non-iron varieties). The geological source bodies are thought to be located between 177.389 and 991.626 meters deep, according to the Euler depth solution. This shows that during the orogenic process, a sequence of strong deformations were present alongside the Toro.***

I. INTRODUCTION

Geophysics is the study of the earth's interior, atmosphere, and terrestrial space through the application of physical laws and precise physical measurements. The magnetic approach is the most used geophysical technology currently available. Moghaddam, 2015. This is largely attributable to how cheaply and easily magnetic data can be acquired. There are several uses for aeromagnetic data, including mineral and oil and gas exploration. Geothermal research by Chinwuko et al. (2012), Nwosu (2013), and Abraham et al. (2014) Aeromagnetic survey is a common type of geophysical survey which is carried out using a magnetometer aboard or towed behind an aircraft Burger et al.,(2006). The principle is similar to a magnetic survey carried out with a hand-held magnetometer, but allows much larger areas of the Earth's surface to be covered quickly for regional reconnaissance. The aircraft typically flies in a grid-like pattern with the height and line spacing determining the resolution of the data (and cost of the survey per unit area). As the aircraft flies, the magnetometer measures and records the total intensity of the magnetic field at the sensor, which is a combination of the desired magnetic field generated in the Earth as well as tiny variations due to the temporal effects of the constantly varying solar wind and the magnetic field of the survey aircraft. By subtracting the solar, regional, and aircraft effects, the resulting aeromagnetic map shows the spatial distribution and relative abundance of magnetic minerals (most commonly the iron oxide mineral magnetite) in the upper levels of the Earth's crust. Because different rock types differ in their content of magnetic minerals, the magnetic map allows for a visualization of the geological structure of the upper crust in the subsurface, particularly the spatial geometry of bodies of rock and the presence of faults and folds. This is particularly useful where bedrock is obscured by surface sand, soil, or water. Aeromagnetic data were once presented as contour plots, but now they are more commonly expressed as thematic (colored) and shaded computer generated pseudo-topography images. The apparent hills, ridges and valleys are referred to as aeromagnetic anomalies.

Aeromagnetic anomalies are the apparent hills, ridges, and valleys. The form, depth, and characteristics of the rock masses causing the anomalies can be inferred by a geophysicist using mathematical modeling Burger et al., (2006). One of the most cost-effective geophysical methods for defining subsurface structures is the magnetic method (Sultan and Josef, 2014). According to Burger et al. (2006), aeromagnetic anomaly maps typically show lateral fluctuations in the earth's magnetic field. These fluctuations are a result of structural modifications, changes in magnetic susceptibility, or residual magnetization.

It was found that igneous and metamorphic rocks had larger magnetic qualities (intensity and susceptibility) than sedimentary rocks, which have lower magnetic properties. As a result, aerial magnetic surveys can be used to directly detect magnetic minerals or map the geologic structure on or inside the basement rocks. Modern geophysics includes airborne geophysical surveys, which are of utmost importance. Airborne surveys enable faster and typically less expensive covering of vast areas when compared to ground surveys Olowofela et al., (2012).

A. Location of the Area

The area is about 60kilometer southwest of Bauchi Capital of Bauchi State, between metric grid coordinates between 1080000N to 1140000N and 500000E to 560000E which corresponds to Latitudes $9^0$40'00"N to $10^0$10'00"N and Longitudes $9^0$0'0"E to $9^0$40'0'E (Fig. 1).

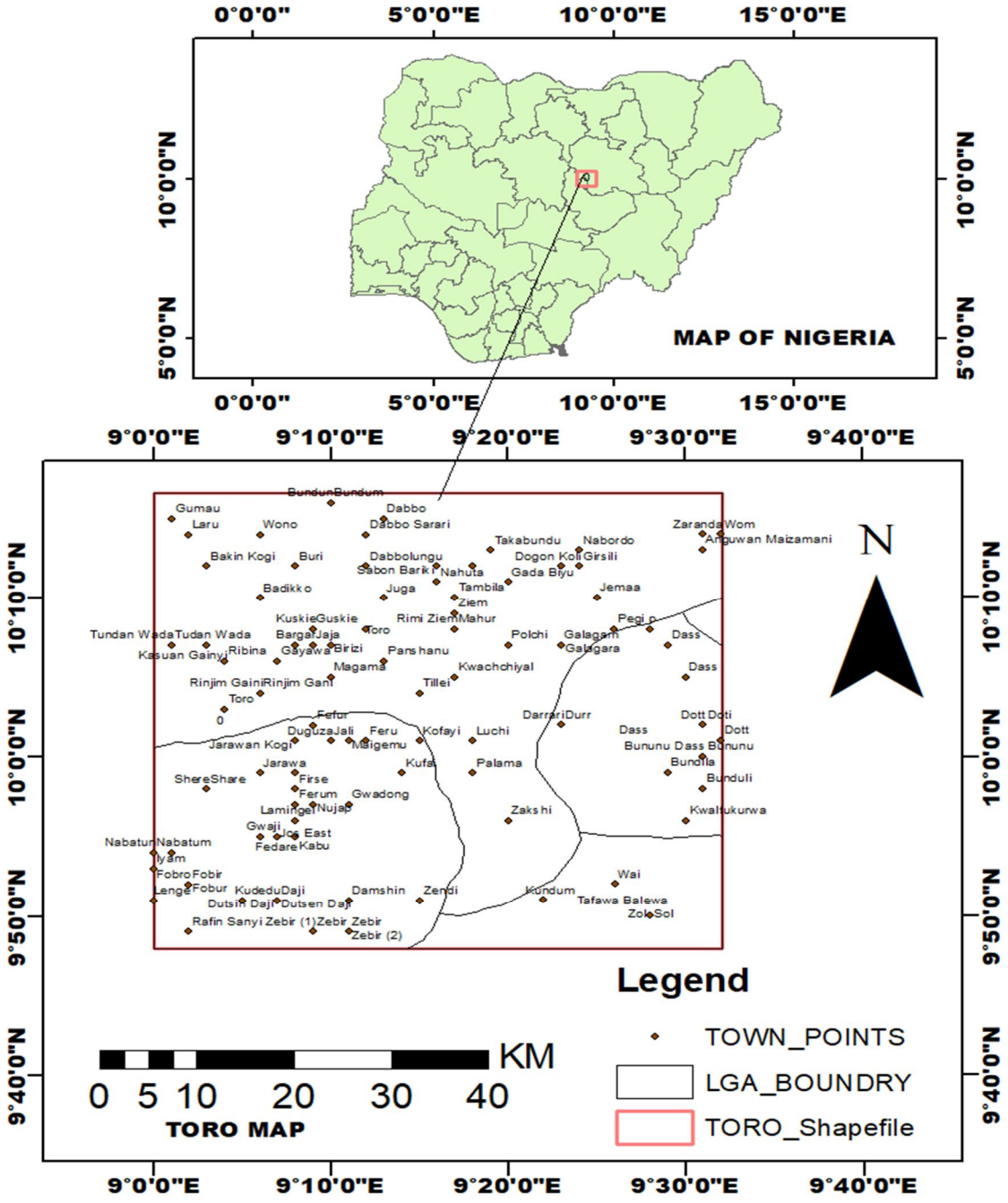

Figure 1; the study Area map

B. Geology of Kwandonkaya

The Kwandonkaya Complex is entirely composed of granitic rock, and there is no trace of any previous volcanic activity. Both of the two most significant units are biotite-granite with different grain sizes and textures. Due to the third biotite-granite's extensive textural variation and probable hybridization of the two previous phases, its contacts with these intrusions are largely ambiguous and transitional (Bul 32 Vol. I). on the roof pendants of Ziem Peak and Dabbolungu, respectively, are remnants of two older intrusions of hornblende-fayalite and hornblende-biotite-granite. The current arrangement of the Dagga Allah porphyry and its accompanying dyke swarms suggests that they have been substantially covered by the later granites of the Kwandonkaya Complex, and it is possible that the pendant of hornblende-fayalite-granite on Ziem Peak was once a component of a horizontal sheet associated with the porphyry (fig. 2). As an overview, below is the complex's cycle of intrusions:

1) Panshanu biotite
2) Porphyry biotite-granite
3) Medium-grained biotite-granite
4) Panshanu biotite-granite
5) Hornblende-biotite-granite
6) Hornblende-fayalite-granite

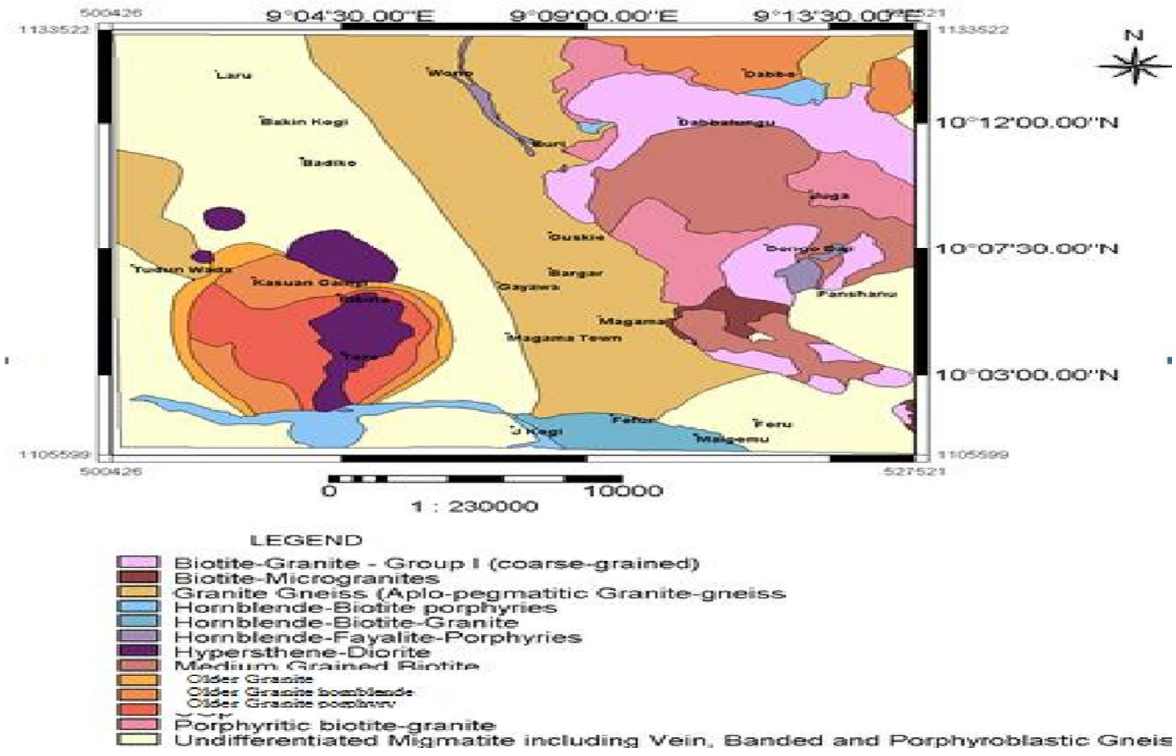

Figure 2: Toro and Environs source showing a digitalized geological map (Aluwong 2017)

II. MATERIALS AND METHODS

A. Materials

The materials include: Total Magnetic Intensity map (Aeromagnetic map) covering Toro sheet 148(1:100 000), Geologic map covering Toro sheet 148 (1: 100 000), Study area map covering Toro area as well as the software include: Geosoft® Oasis Montaj™ ArcGIS, Micro soft word and Excel

B. Method

1) Data Acquisition

The Nigerian Geologic Survey Agency (NGSA) provided the High Resolution Aeromagnetic (HRAM) data of Toro (Sheet 148), which covers the area under examination. Half-degree sheets of data were created using information gathered at a height of 80 meters along NE-SW flight lines that were roughly 500 meters apart.

2) Data Analysis

The residual magnetic field grid was subjected to a variety of filtering procedures in order to facilitate understanding. These filtering methods were chosen because they most clearly define and support the work's study interest. Analytical signal, total horizontal derivative, and Euler De convolution techniques are some of the methods. Below is a brief discussion of the theories underlying these methods.

3) Analytic Signal

The analytical signal technique is based on the use of the first derivative of magnetic anomalies to infer source properties and pinpoint the locations of geologic boundaries like contacts and faults. The definition of the Analytic Signal (AS) amplitude, which is provided by Roest (1992, is the square root of the squared sum of the vertical and the two horizontal first derivatives of the magnetic field anomaly T.

$$|\mathbf{AS}(x,y)| = \sqrt{\left(\frac{\partial T}{\partial x}\right)^2 + \left(\frac{\partial T}{\partial y}\right)^2 + \left(\frac{\partial T}{\partial z}\right)^2} \quad \ldots\ldots\ldots\ldots \quad 1$$

The Analytic Signal approach has the benefit of defining source positions despite any residual magnetization in the sources. It is therefore unaffected by the magnetization's orientation, according to Milligan (1997). The anomalous source body borders and corners are identified by maxima (ridges and peaks) in the derived analytic signal of a potential field anomaly map.

4) Total Horizontal Derivative

The horizontal gradient method is a quick and easy way to determine where bodies will make touch at depth. The Total Horizontal Derivative (THD) magnitude, if T is the magnetic field, is given by:

$$\mathbf{THD} = \sqrt{\left(\frac{\partial T}{\partial x}\right)^2 + \left(\frac{\partial T}{\partial y}\right)^2} \quad \ldots\ldots\ldots\ldots\ldots\ldots\ldots 2$$

Under the following presumptions, this function yields a peak anomaly above magnetic connections:

a) the regional magnetic field is vertical;
b) the magnetizations are vertical;
c) the contacts are vertical;
d) the contacts are isolated; and
e) The sources are thick. Peaks may move away from contacts as a result of violations of the first four presumptions. Secondary peaks parallel to the contacts may result from breaking the fifth assumption. Since only the two first-order horizontal derivatives of the field need to be calculated, the horizontal gradient method's primary benefit is its minimal sensitivity to data noise Phillips (1998).

III. EULER DECONVOLUTION

A popular method for depth assessment and delineating a range of geologic features in three dimensions is called the Euler De Convolutions. It is based on the Euler homogeneity equation (3), which connects the position of the sources to the gradient components of the potential field (gravitational or magnetic), and as well as the degree of homogeneity N, which is understood as a structural index. (1998, Phillips).

$$(x - x_o)\frac{\partial T}{\partial x} + (y - y_o)\frac{\partial T}{\partial y} + (z - z_o)\frac{\partial T}{\partial z} = N(B - T)$$

……3

Where T is the total field at (x, y, z) and B is the regional value and N is the structural index. Assuming various measurement point and known N, the above equation can be solved with least squares procedure for unknowns x_0, y_0, z_0 and B.

The structural index N is a crucial element in the Euler equation. This homogeneity factor connects the source's position to the magnetic field's gradient components. It has been demonstrated that a bad choice of the structural index results in a diffuse solution of source locations and significant errors in depth estimates. According to Thomson (1982), a correct N results in the tightest clustering of the Euler solutions around the target geologic structure. The degree of homogeneity of potential fields and structural indicators of Euler De Convolution are more thoroughly discussed by Thompson (1982).

IV. RESULTS AND DISCUSSION

A. *The Total Magnetic Intensity*

Fig. (4.1) shows a map of the study area's total magnetic intensity. The map was divided into three main sections, despite the fact that there are minor depressions all throughout the region. The blue and green portions of the southwest and a few northwest regions stand for the low and moderate magnetic values, respectively. Red to pink colors are used to signify high magnetic intensity values, which are predominate in the southeast toward the north east and west half of the study area. The strong magnetic values that dominate the study area's northern and southern half are probably caused by the near-surface igneous rocks' high magnetic sensitivity. The low amplitude TMI results are most likely caused by the sedimentary rocks.

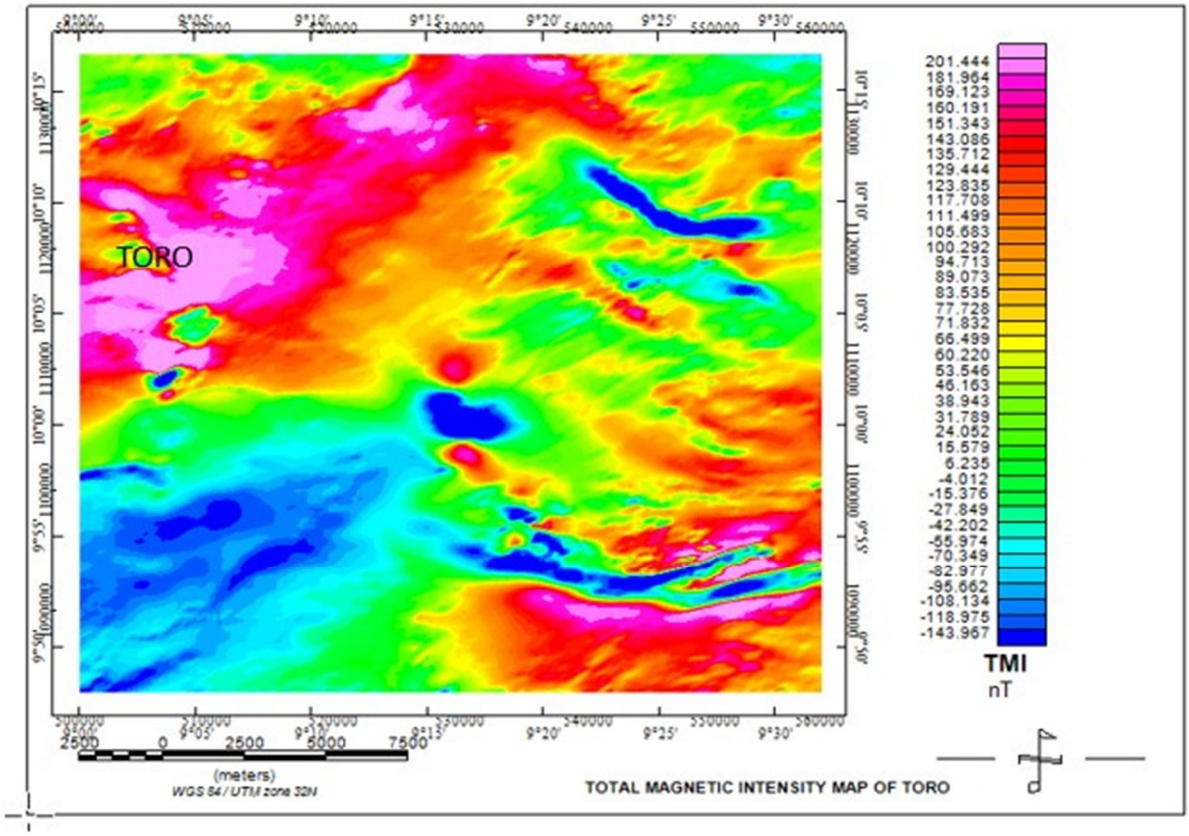

Figure 4.1 TMI map of the study area

B. *Residual Magnetic Intensity Map*

The residual magnetic intensity map produced in this investigation using polynomial fitting using Montaj software is shown in Figure 4.2. The readings of the magnetic field's strength range from -166.110 to 172.595 nT while negative magnetic intensity values are distributed across the study area, they are more pronounced in the northeast-southwest and north central regions. Positive magnetic intensity values are more pronounced in the southern and western portions of the study area. Additionally, there are sporadic positive magnetic intensity values in the eastern part. Positive magnetic intensity values migrate northwest to southeast in the examined region, while negative magnetic intensity values move NE to SW. The enhanced magnetic intensity data were brought on by the intruding body that entered the magnetic field.

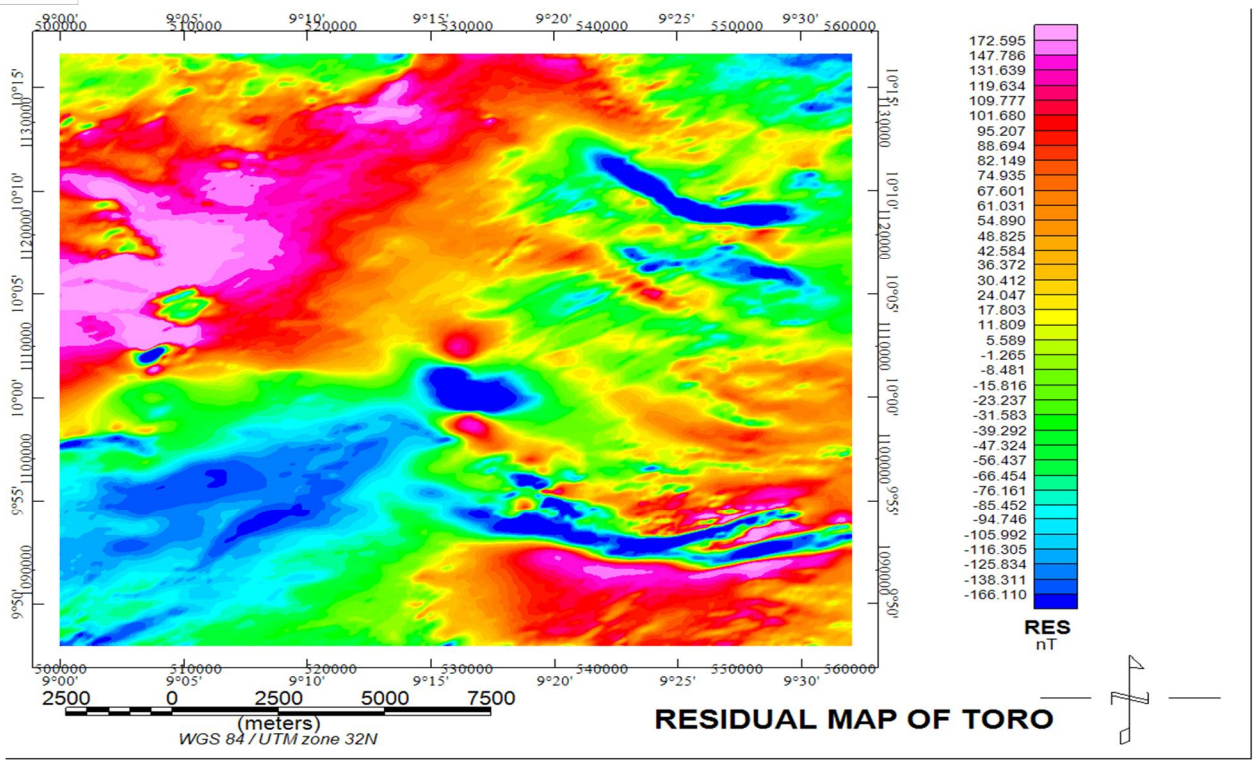

Figure 4.2 the Residual map of the study area

C. The Regional Map

The polynomial fitting method of the first order was used with the Oasis Montaj version 8 to begin the interpretation of the magnetic data, and the regional-residual separation technique was used on the TMI to filter the regional component, which originates due to deep seated sources, from the residual component, which is related to local shallow structures.

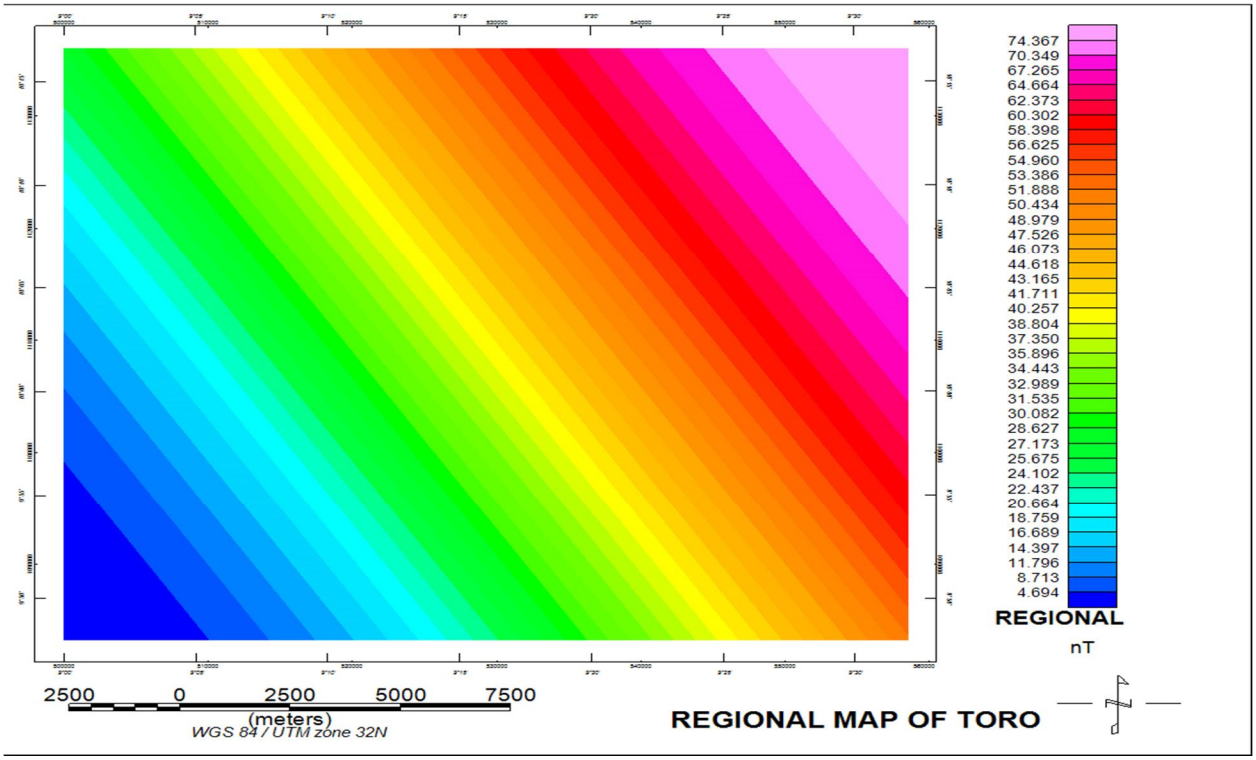

Figure 4.3 the regional map of the study area

D. The RTE map

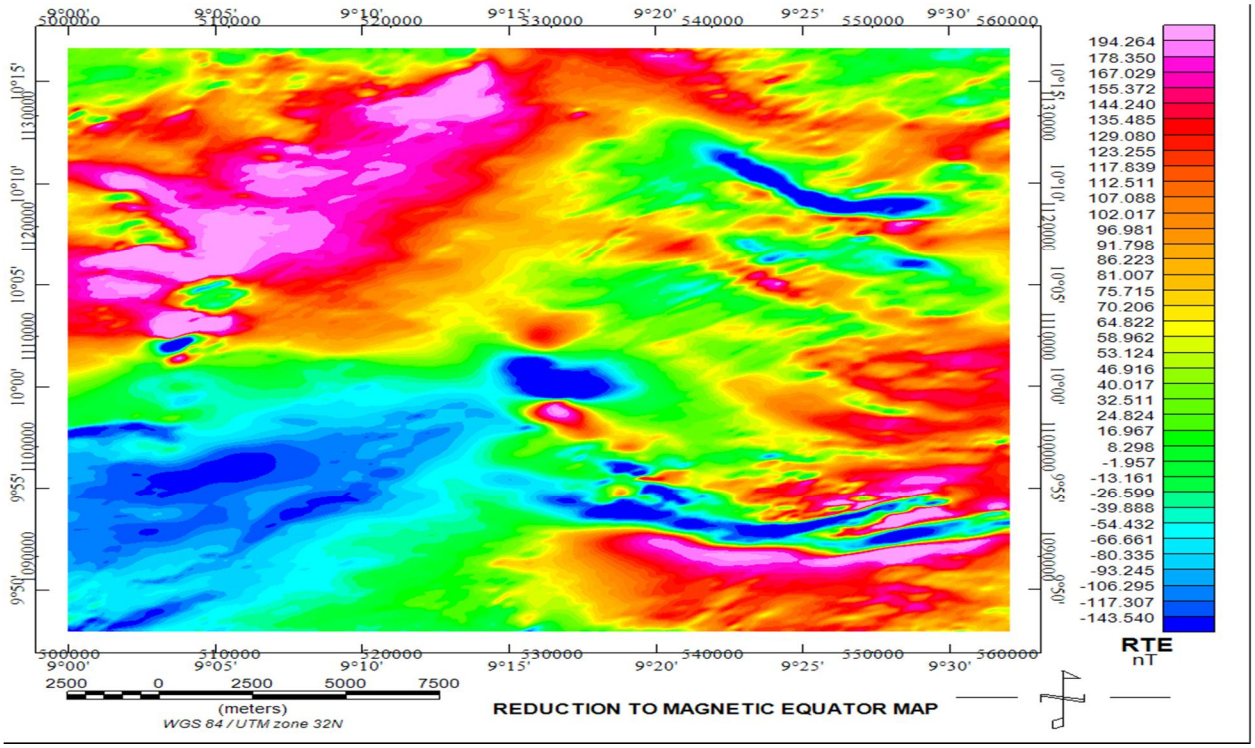

Figure 4.4 the RTE map of the study Area

E. Analytical Signal

Analytical Signal Map figure (4.5) shows the variation in the amplitude (both high and low) of the anomalies. It was observed that the high amplitude anomaly is as a result of intrusive bodies into the sedimentary structure, and the high amplitude anomaly is attributable to wide variation in susceptibility of rock-units in zones of fracturing, shearing and faulting. While the low amplitude anomaly was associated with sedimentary region which is the area of interest in this study. The high amplitude anomaly trends North East – South East (NE-SE) while the low amplitude anomaly trends Northwest-Southwest (NW-SW). This distinguishes the area into regions of magnetic boundaries, intermediate structures and basements under the influence of thick sedimentation, it shows the types of outcrops present.

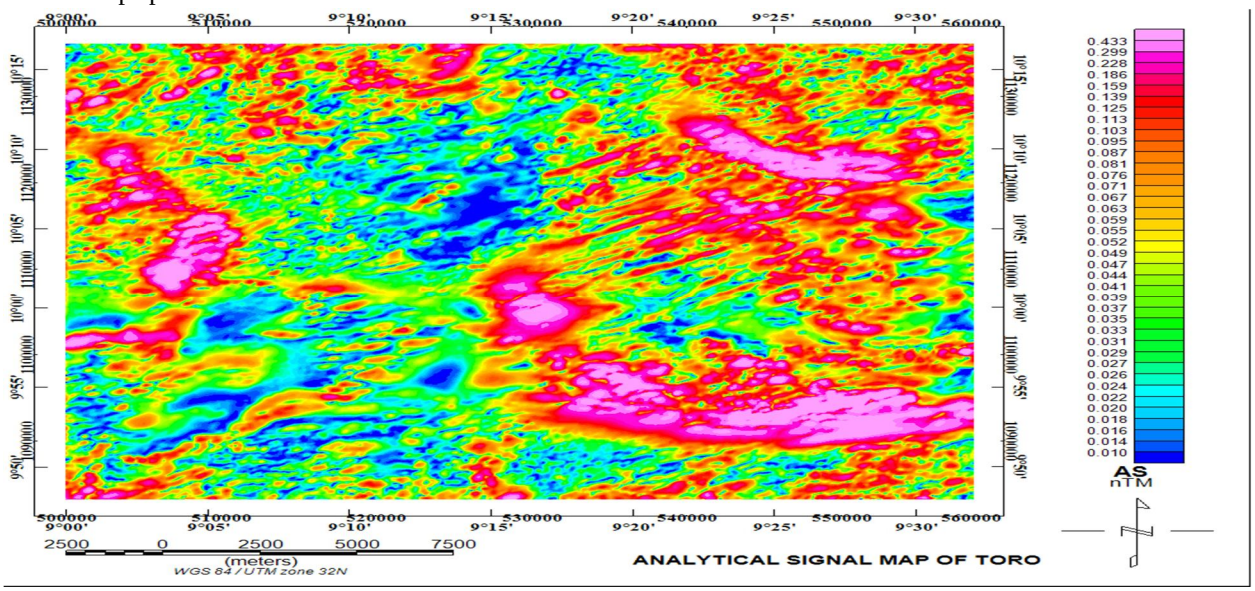

Figure 4.5 the AS map of the study Area

F. The First Vertical Derivative

Demonstrates the first vertical derivative of the study's total magnetic intensity map, which reveals the texture of the total magnetic intensity anomalies. It can be used to locate magnetic lineaments and to more clearly define the boundary between lithological units. The lines shown on the map show the location and orientation of faults, fractures, and lineaments.

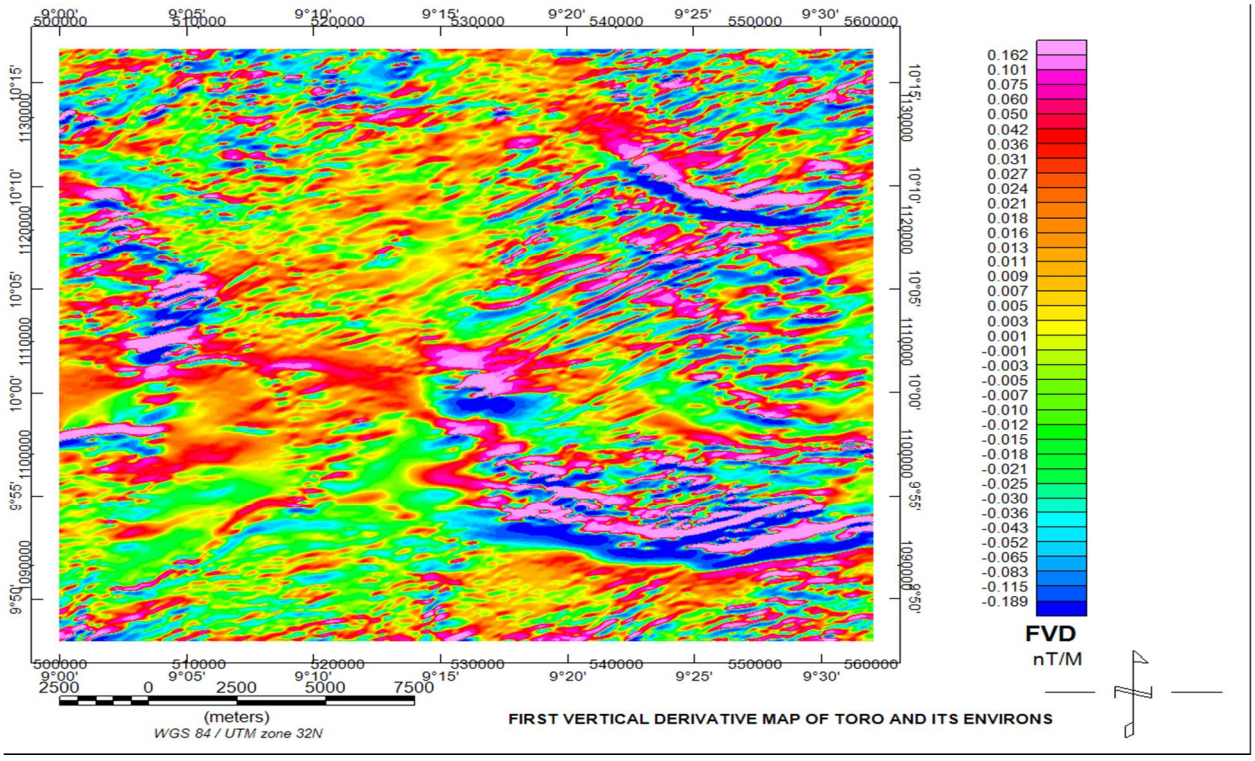

Figure 4.6 the FVD map of the study area

G. Total Horizontal Derivative Technique

The anomalies observed on the Total Horizontal Gradient Map figure (4.7) correspond largely to that observed from the analytic signal Figure (4.5). The horizontal gradient method provides contact locations that are continuous and thin. The horizontal gradient values ranges from -0.972 to 0.986 nT/m and shows a large contrast in magnetic susceptibility along geologic contacts. From figure (4.8), magnetic lineaments within the area of study where automatically extracted using the CET Analysis Oasis Montaj software and the result is shown on Figure (4.8).

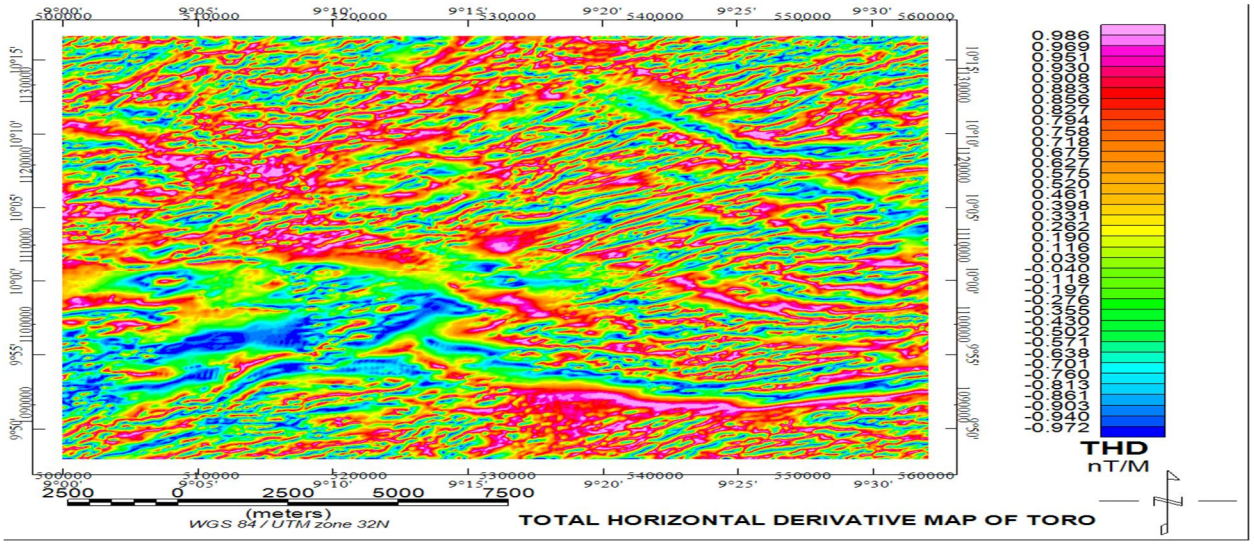

Figure 4.7 the THD map of the study area

H. Centre for Exploration Targeting (CET)

A way of automating lineament delineation is center exploration targeting. Intriguingly, the CET results figure (4.8) show a stronger correlation between the lineaments depicted on the FVD and what was seen on the first vertical derivative Figure (4.6). The fact that the Center exploration targeting was successful in extracting the coordinates where these lineaments were seen is an added benefit. Figure (4.6) illustrates the coordinates of these significant structures and lineaments that illustrate the degree of mineralization of particular relevance are the lineaments controlled by the three main trend lines. NE-SE, NW-SE, and N-S directions make up these features trends.

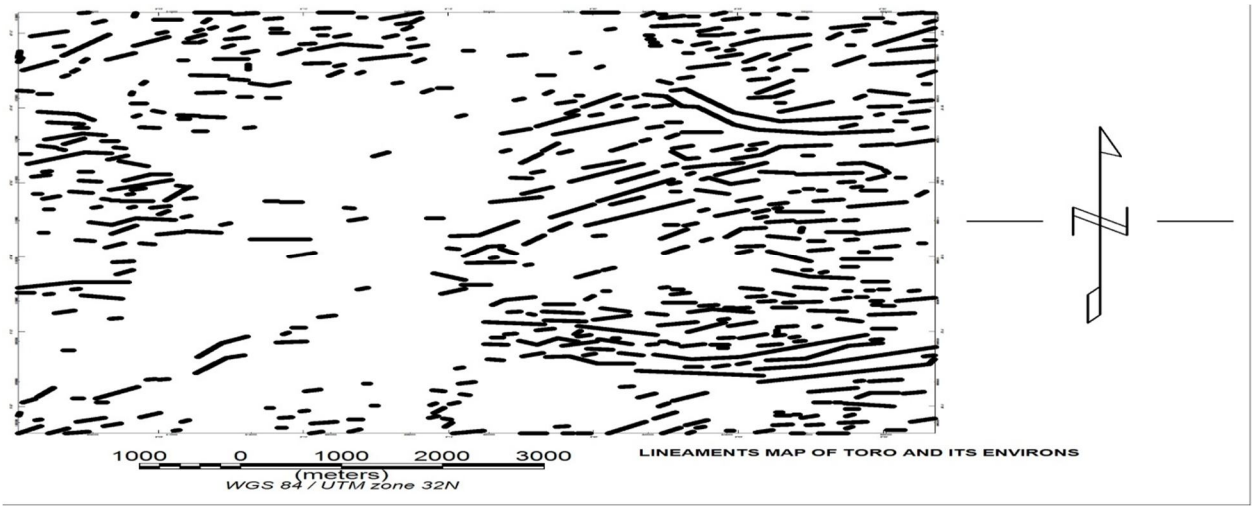

Figure 4.8 the lineament map of the study area

I. Interpretation Of 3D Euler Deconvolution

The structures in the research area's northwest and southwest exist at relatively deeper depths than those in other areas, according to the Euler solutions. The variation in depths along the fault zones is indicated by the linear clustering of various depth solutions. In the northwest and southwest, there are a lot of constructions at depths greater than 373 meters. From the research areas middle section to its northeastern corner, shallow solutions were seen. These solutions, which have a depth of less than 320 m and trend NE-SE and NW-SW, likewise fall on the study area's complicated basement terrain. These patterns can represent faults on or in the basement.

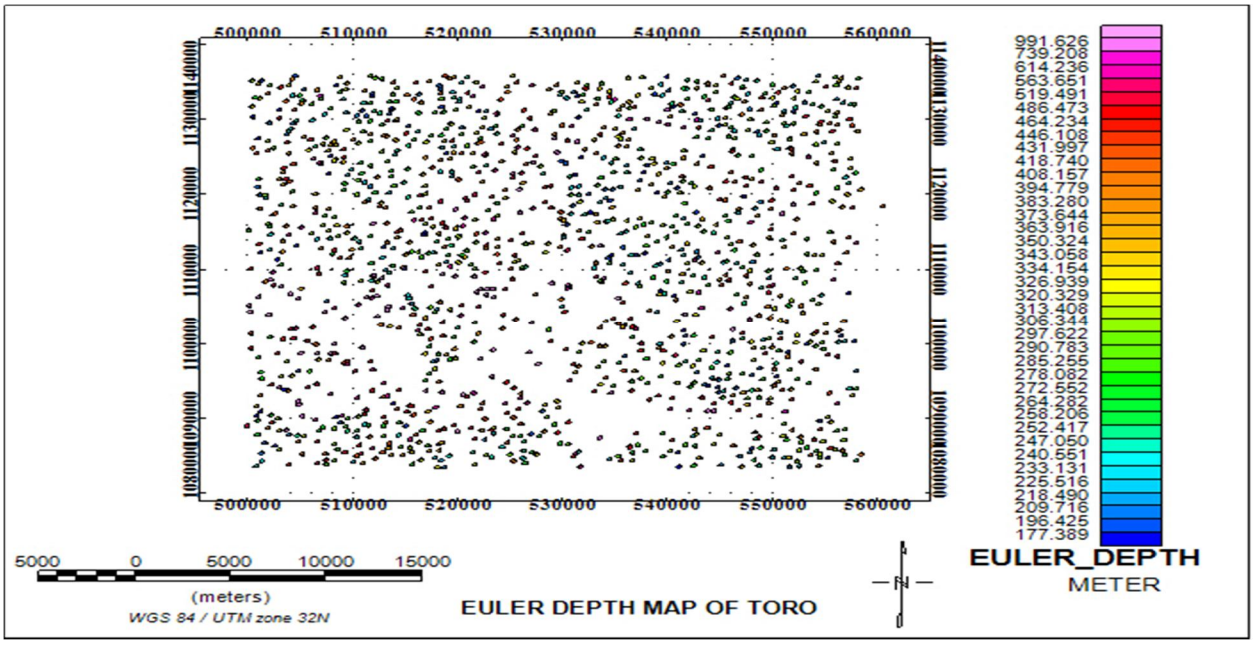

Figure 4.9 the Euler depth map of the study area

V. CONCLUSION

The subsurface geophysical and geological structures of the research region have been understood through the processing and interpretation of the aeromagnetic data. According to the digital aeromagnetic map, the Toro and its surroundings, which are composed of Basement complex rock types, are particularly rich in iron mineralization. The lithological map can be seen reflected in the lineament map, which shows clusters of lineament around significant fault or fractured zones. The depths to geological structural model Dikes have been clearly proven to be between 177.389 and 991.626 meters, and the Analytical map and the Total horizontal magnetic map showed positive correlations with the iron mineralization map. Additionally connected with each other and primarily going NE-SE in the region are the first vertical derivative and structural lineaments. As a result, there are large variations in the depth to the magnetic source bodies along main lineaments, which range from 0-2000 m.

REFERENCES

[1] Abraham EM, Lawal KM, AmobiChigozieEkwe AC, Alile O, Murana KA, et al. (2014) Spectral analysis of aeromagnetic data for geothermal energy investigation of Ikogosi Warm Spring-Ekiti State, South-Western, Nigeria. Geothermal Energy 2014 2: 6.
[2] Aluwong K. C., Bala, D. A., Kamtu, P. M. and Nimchak, R. N.IOSR Journal of Applied Geology and Geophysics (IOSR-JAGG) E-ISSN: 2321–0990, p-ISSN: 2321–0982.Volume 5, Issue 3 Ver. I (May. - June. 2017), PP 34-4
[3] Burger R.H., Sheehan, A.F., and Jones, C.H. (2006). Introduction to Applied Geophysics Published by W.W. Norton. 600 pages.
[4] Chinwuko AI, Onwuemesi AG, Anakwuba EK, Onuba LO, Nwokeabia NC (2012) Interpretation of aeromagnetic anomalies over parts of upper Benue trough and Southern Chad Basin, Nigeria. Adv in App Sci Res 3: 1757-1766.
[5] Dolmaz MN, Hisarli ZM, Ustaomer T, Orbay N (2005) Curie point depths based on spectrum analysis of aeromagnetic data, West Anatolian Extensional Province, Turkey. Pure Appl Geophys 162: 571–590
[6] Milligan PR, Gunn PJ (1997) Enhancement and presentation of airborne geophysical data. J Aus Geol Geophys 17: 63-67.
[7] Moghaddam MM, Sabseparvar M, Mirzaei S, Heydarian N (2015) Interpretation of aeromagnetic data to locate buried faults in north of Zanjan Province, Iran. J Geophys Remote Sensing 4: 143.
[8] Nwosu OB, Onuba LN (2013) Spectral re-evolution of the magnetic basement depth over part of middle Benue Trough Nigeria using HRAM. Int J Sci Technol Res 2: 97-111.
[9] Obande GE, Lawal KM, Ahmed LA (2014) Spectral analysis of aeromagnetic data for geothermal investigation of Wikki Warm Spring, north-east Nigeria. Geothermic 50: 85–90.
[10] Olowofela, J.A., Akinyemi, O.D., Idowu, O.A., Olurin, O.T. and Ganiyu S.A. (2012). Estimation of Magnetic Basement Depths beneath the Abeokuta Area, South west Nigeria from Aeromagnetic Data using Power Spectrum. Asian Journal of Earth Sciences 5(2), 70-78.
[11] Phillips JD (1998) Processing and interpretation of aeromagnetic data for the Santa Cruz Basin-Patahonia Mountains Area, South-Central Arizona. U.S. Geological Survey Open-File Report, Arizona, 2002–98.
[12] Roest WR, Verhoef J, Pilkington M (1992) Magnetic interpretation using 3-D analytic signal. Geophys 57: 116-125.
[13] Sultan, A.S.A and Josef, P. (2014). Delineating groundwater Aquifer and subsurface structures using Integrated Geophysical interpretation at the Western part of Gulf of Aqaba, Sinai, Egypt. International Journal of Water Resources and Arid Environments 3(1), 51-62
[14] Thomson DT (1982) EULDPTH: A new technique for making computer-assisted depth estimates from magnetic data. Geophys 47: 31–37.

.

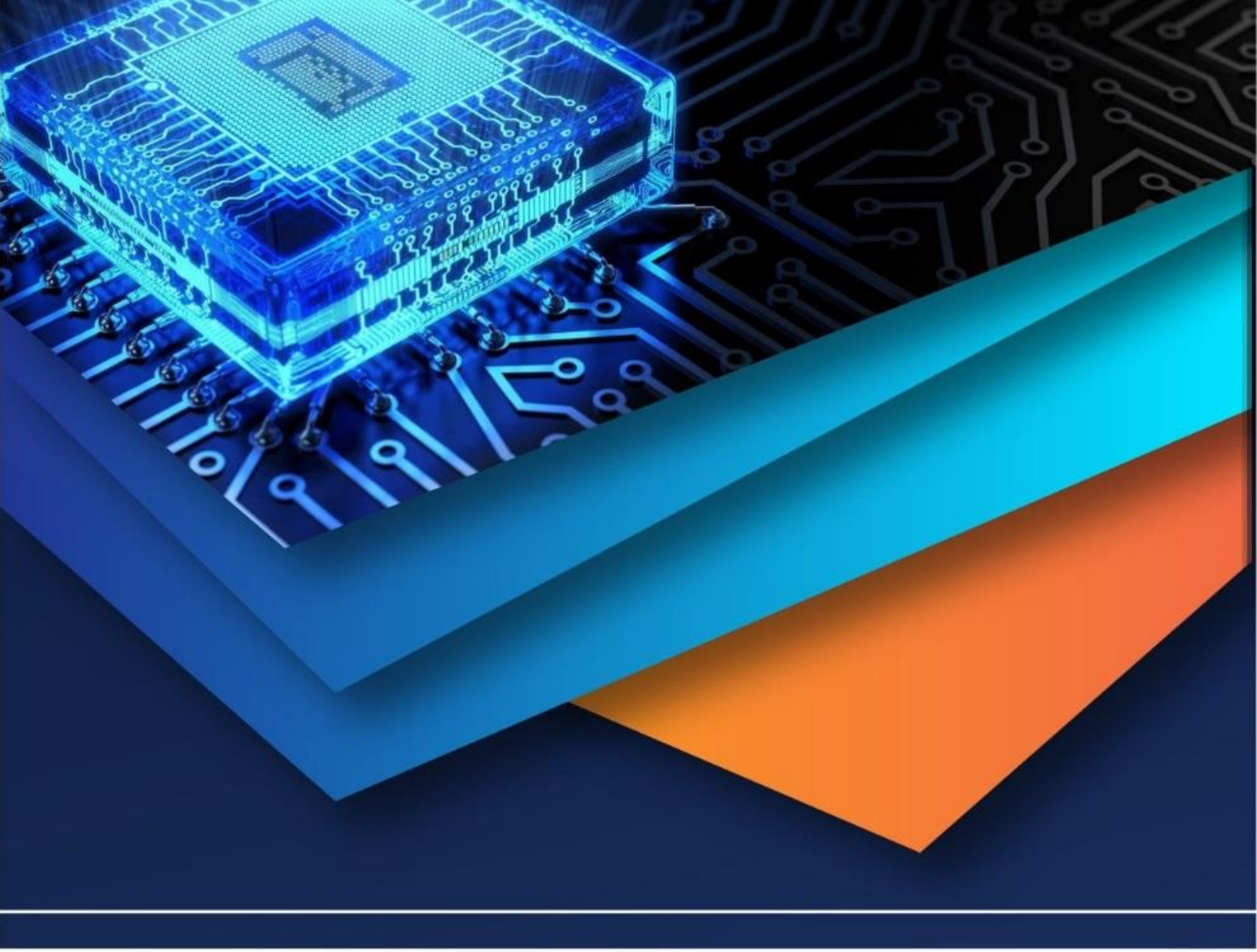

10.22214/IJRASET

45.98

IMPACT FACTOR: 7.129

IMPACT FACTOR: 7.429

INTERNATIONAL JOURNAL FOR RESEARCH

IN APPLIED SCIENCE & ENGINEERING TECHNOLOGY